DOI : https://doi.org/10.56452/7-2-554

ISSN: 0974-5823 Vol. 7 No. 2 February, 2022

*International Journal of Mechanical Engineering*

# A Coded-Excitation System Based On Filters for Fast Ultrasonic Imaging

**Sakshi Painuly**
Asst. Professor, School of Computing, Graphic Era Hill University, Dehradun, Uttarakhand India 248002,

**Abstract:**

Because of its many useful properties, ultrasonography has won over both patients and doctors as a reliable diagnostic tool for medical investigations. Due to a signal-dependent noise known as "Speckle," the applications of ultrasound are severely constrained. Because of this background noise, it might be difficult for doctors to objectively evaluate ultrasound results. There are two primary types of ultrasound despeckling methods: spatial domain and transform domain. Therefore, the primary goal of this study is to create novel spatial and transforms domain filters for superior edge-preserving denoising of ultrasound pictures. WT-FBNF is a wavelet-based thresholding filter that employs quick bilateral and Neigh ShrinkSure filtering on both the approximation and detail bands. Both NS-MAP and SNIGS-MAP filers are types of denoising methods known as coefficient modelling. To achieve superior image decomposition, DST is used in lieu of WT in both filters, and MAP estimation is used to generate noise-free shearlet coefficients. Experiments were performed using both simulated and actual ultrasound images to assess the effectiveness of each filter proposal.

**Keywords: Ultrasound, shearlet, Neigh ShrinkSure filter, bilateral**

## Introduction

Medical imaging is a valuable tool for examining the structure and function of the human body from the inside. The diagnostic process for many illnesses and conditions is aided by medical imaging, which is used by physicians and medical professionals. Computed tomography (CT), magnetic resonance imaging (MRI), nuclear medicine, radiology, and Ultrasonography are all utilised for this purpose. These many imaging techniques all come with their own set of advantages and disadvantages. CT scans provide high-resolution pictures of skeletal structures, but they expose patients to radiation, which has potential health risks [1]. MRI scans, on the other hand, have no such risks. Although magnetic resonance imaging (MRI) may provide high-quality cross-sectional pictures of bones and soft tissues, it is prohibitively costly, time-consuming, and risky for patients with implanted electronic cardiac devices [2]. In addition, patients and doctors have come to consider ultrasonography as a reliable diagnostic tool for medical investigations because to its many benefits, including being non-ionizing, non-invasive, safe, flexible, and affordable [3]. It also has the benefit of portability, making it convenient for patients in critical care settings to utilise while lying in bed. Real-time imaging is also often used to monitor foetal growth and detect tumours in the abdominal organs, as seen in the medical care of pregnant women. Medical ultrasonography not only captures pictures of bones, hard tissues, and soft tissues, but also the flow of blood inside blood vessels [4]. Ultrasound

imaging also has many other benefits. Inadequate signal-to-noise ratio (SNR) and the presence of a signal-dependent, multiplicative noise source ('Speckle') restrict the imaging modality's use. All coherent imaging modalities, including ultrasound (US), synthetic aperture radar (SAR), and laser, continue to struggle with the issue of speckle. Because speckle is a multiplicative kind of noise, it makes the picture seem grainy. The interference between the original sound and the reflected echo causes this background buzzing and humming. Speckle noise worsens US images by hiding low-contrast lesions and other tiny features and edges [5–7]. US pictures have greater granularity at low acoustic frequencies compared to high acoustic frequencies [8], which is a function of the transducer frequency. The subjective evaluation of US data is complicated by speckle, which presents a difficulty to medical professionals. Furthermore, picture post-processing tasks like segmentation and pattern identification become challenging when speckle is present [9]. In order to enhance the diagnostic capability of medical ultrasound imaging and the ease with which it may be seen, speckle suppression is crucial. Different types of human tissue affect the transmission of ultrasound waves in unique ways. As they travel across space, US waves may be reflected, refracted, scattered, or absorbed [10]. When US waves with an incidence angle of 90 degrees hit the border between two tissues with varying acoustic impedances, part of the waves are reflected back towards the transducer. When the angle of incidence is not 90 degrees and there is a mismatch in the acoustic impedances, refraction occurs. US photos are corrupted by the refraction phenomena. When ultrasound waves collide with things that are on the order of the wavelength or smaller, the waves are scattered. The scattering of a wave, and in what direction and to what extent, depends on the nature and size of the tiny item. US waves that penetrate deeper into the body are severely dampened and absorbed, resulting in thermal effects. However, the echoes, which are the wave's reflected components, are what the transducer picks up and uses to create a picture.

**Speckle Noise**

Speckle is an annoying artefact when using coherent systems like ultrasound, synthetic aperture radar, or laser. Interference between the transmitted wave and the backscattered wave results in speckle noise. The target surface returns a backscattered wave to the sensor at unpredictable times. Speckle noise is the result of destructive and constructive interference caused by the superposition of these waves. The screen displays a granular pattern due to this noise. The low and high acoustic frequency speckle noise patterns are shown in Figure 1. Tissue type, depth, and transducer properties all have a role in how visible the speckle is. The frequency at which the transducer operates also determines the quantity and size of each granular pattern. Due to poor longitudinal and lateral decisions, brighter spots look bigger when a low-energy US beam is employed for imaging, creating a coarser appearance in the pattern of speckles [15]. High frequency US beam, on the other hand, has higher axial and lateral resolutions, allowing for a more nuanced depiction of the dark and brilliant pattern (Figure 1). Speckle noise may be modelled using a multiplicative random-noise process. Medical ultrasound pictures exhibit one of three distinct types of speckle patterns. The amount of scatterers per resolution cell, their geographic distribution, and other US system features are used to describe these groups. [5]-[7].

DOI : https://doi.org/10.56452/7-2-554

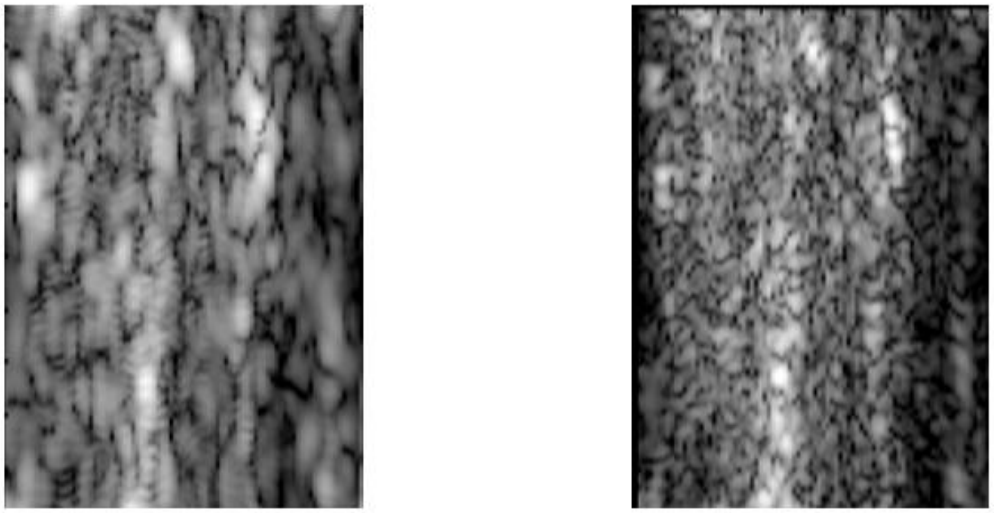

(a) (b)

**Figure 1:** Speckle noise pattern **(a)** at low acoustic frequencies, **(b)** at high acoustic frequencies

**Literature Review**

**Xun Lang et.al.,(2021)** Since non-contrast ultrafast Doppler imaging of blood flow relies on the discriminating between tissue and blood motion, clutter filtering technology has garnered a lot of interest thanks to the swift growth of ultrafast ultrasound imaging that utilises the unfocused transmission of plane-wave. Singular value decomposition (SVD), a popular method of clutter filtering, is a black-box technique, and it is possible that blood flow or tissue activities would be disrupted if any singular vector related to the first singular values were directly rejected. Blood flow imaging and velocity profile estimation using signals collected from the carotid arteries of 10 healthy human subjects are evaluated using the proposed adaptive clutter disapproval technique utilising the fast multivariate empirical mode decomposition (FMEMD), and compared to the high-pass filter (HPF) and SVD. The results show that the suggested approach outperforms the state-of-the-art methodologies, particularly when it comes to separating blood flow and tissue signals close to vessel walls.

**Iman Taghavi et.al.,(2021)** One of the most therapeutically relevant metrics is velocity. Multiple investigations have shown that this parameter may be visualised using velocity maps utilising super-resolution (SR) ultrasound imaging. However, it might be difficult to manually separate the velocity estimates for arteries from veins. Four healthy Sprague-Dawley rat kidneys were utilised to automatically classify arterial and venous blood velocities in SR images, and the differences in these velocities throughout the medullary regions were assessed. The measurements were taken using a customised version of the bk5000 scanner (BK Medical, Herlev, Denmark) in conjunction with a BK 9009 linear array probe using a pulse amplitude modulation technique. A SR processing pipeline was used to analyse ten minutes' worth of 54 fps B-mode and contrast pictures. Arterial and venous blood flow were identified in the micro-bubble trajectories using rough anatomical labelling. Separation of data was seen in the velocity estimations of outer medulla arterioles and venules in all rats. This distinction was shown to be statistically significant using the Wilcoxon test (p=0.002). Median

velocities in the OM arterioles and venules were anticipated to be 0.84 0.09 mm/s and 0.70 0.07 mm/s, respectively, based on the study's sample size and t-distributions, respectively. The findings demonstrated the automatic differentiation of blood flow in the outer medulla arterioles and venules of rat kidneys based on anatomical knowledge of the renal vasculature.

**Nans Laroche et.al.,(2021)** The purpose of this work is to discuss nondestructive testing (NDT) in the context of high-resolution ultrasonic image reconstruction using Full Matrix Capture (FMC) data. Data and the ultrasonic model from the time domain are linearly beamformed into the picture domain to lessen the computational burden. Non-stationary and color-coded noise are introduced to the model, leading to an interpretation as a shift-variant convolution process. To smooth down the spatial fluctuations in the resultant point spread function, an interpolation approach is developed. A similar methodology is used to suggest and implement an approximate whitening filter in the forward model. Both structures therefore provide quick calculations with constrained memory. Minimising the least-squares data misfit error is how deconvolution is carried out, using a penalization term that gives preference to sparsity and spatial continuity in the final pictures. Simulation results are very similar to those obtained by inverting raw FMC data, demonstrating the computational efficiency of the suggested method. Finally, lab data are used to evaluate an aluminium block with tiny, closely spaced holes bored onto the side. Flaws with diameters six times smaller than the wavelength and separated by a distance three times less than the resolution limit specified by the Rayleigh criteria may be successfully detected and separated.

**Research Objectives**

For the last three decades, medical professionals have relied heavily on ultrasound imaging as a means of diagnosis. US pictures are commonly employed for the assessment of a broad range of health concerns because of the many advantages of this imaging modality over other imaging modalities. However, a signal-dependent noise known as "speckle" degrades the clarity of medical US pictures. This multiplicative noise manifests itself in US photos as a granular texture. There are two primary categories of speckle denoising methods: spatial domain methods and transform domain methods. Although several studies have been conducted on US despeckling in both areas, it was shown that there is always room for improvement. Therefore, either the current US denoising algorithms need to be modified or some new denoising algorithms need to be invented to enhance denoising of medical US imaging. New spatial and transform domain filters for effective speckle noise reduction in US pictures are the primary focus of the proposed study. The suggested filters must meet both of the following conditions at the same time:

1. Proposed filter should be able to perform strong denoising in homogeneous regions.

The proposed filter must be able to maintain sharp edges and other finer features in the denoised picture.

In order to acquire a quantitative and qualitative evaluation of the effectiveness of the filters, extensive testing will be undertaken using both simulated and genuine US photographs after the filters have been constructed according to the required criteria. Visual inspections of the resultant denoised images are used for both quantitative and qualitative assessments..

Despite their widespread use, wavelet-based approaches for reducing speckle noise in US pictures can only deal with discontinuities at single points. In order to achieve more effective denoising of US

pictures, it may be more beneficial to employ different extensions of wavelets, such as ridglets, curvelets, contourlets, ripplets, and shearlets. In this study, we also provide a digital version of the ridgelet transform and a curvelet transform. In this article, we provide a technique in the curvelet domain for reducing speckle noise in US photos. The blocks recovered via spatial filtering of the image's subbands after decomposition are subjected to the ridgelet transform in this technique. The shortcomings of the 2-band wavelet transform are addressed by the M-band ridgelet transform. In this article, we provide a nonlinear technique for reducing speckle noise in log converted US pictures. This technique filters the ripplet coefficients in both the detail band and the approximation band using a block thresholding approach and a bilateral filter. Few Bayesian estimation shrinkage or coefficient modelling techniques based on extensions of wavelets are known in the literature for use in the transform domain. The contourlet coefficients were modelled as NIG distributions by Zhang et al. Because of its thick tails, the NIG distribution is the one used to simulate contourlet coefficients. Estimating the noisy contourlet coefficients using the maximum a posteriori (MAP) method yields noise-free coefficients. The shift variant attribute of the contourlet transform introduces the Gibbs phenomenon, which is mitigated by the use of the cycle spinning method. The coefficients of the log-transformed contourlets that represent the signal and the noise were modelled as coming from a Cauchy distribution and a Maxwell distribution, respectively, by Sadreazami et al. Using MAP estimation, we are able to derive noise-free coefficients. Prior distribution parameters are estimated using ML technique. Linear minimal mean square error (LMMSE) and maximum a posteriori (MAP) estimators were introduced by Argent et al. for use in the nonsubsampled contourlet (NSCT) transform domain. The technique takes use of NSCT coefficients' fourth-order moments. For MAP inference, we use the GGD prior distribution. During US picture denoising, MAP estimator performance is determined to be better than that of LMMSE estimator. Speckle noise reduction for renal US images has been presented by Bama et al. They propose using a mixture of diffusion filtering and MAP estimation of noiseless coefficients in the curvelet domain. Decomposing a picture into its component subbands through the undecimated Atrous curvelet transform. The high-frequency components are filtered out using a shrinkage function, while the low-frequency components are denoised using the PMAD approach. Due to its shift invariance characteristic and compatibility with multi-resolution analysis (MRA), the shearlet transform stands out as the most often used transform. However, no reliable approach that models shearlet coefficients for despeckling of medical US pictures has been published. Because of this, DST presents a promising alternative to the wavelets and other transformations for capturing the directional aspects of US pictures.

**Experimentation and Result Analysis**

The suggested filters, the Segmentation Based NIG Shearlet Map Filter (SNIGS-MAP), were tested in a MATLAB 9.1 environment to see how well they functioned. The suggested approaches are compared to five existing ones: the DWT-Wiener method, the NeighShrinkSure method, the DWT-Cauchy method, the DWT-NIG method, and the DST-NIG without segmentation (DST-NIG-WS) filter. Note that this filter was also built so that it may be compared to the SNIGS-MAP filter. Similar to how SNIGS-MAP is built, the DST-NIG-WS filter does not employ a segmentation of finer-grained features or an adaptive weight function in the MAP expression.

Table 2: PSNR values obtained for synthetic ultrasound images for SNIGS-MAP filter against existing filters

DOI : https://doi.org/10.56452/7-2-554

| Filters | PSNR (dB) | | | | | |
|---|---|---|---|---|---|---|
| | NOISE VARIANCE ($\sigma^2$) | | | | | |
| | Test Image-2 | | | Test Image-3 | | |
| | 0.1 | 0.2 | 0.3 | 0.1 | 0.2 | 0.3 |
| Noisy Image | 20.6811 | 17.8353 | 16.2502 | 16.3160 | 13.6025 | 11.9186 |
| DWT-Wiener[62] | 27.3234 | 23.2669 | 20.1648 | 18.0525 | 15.1252 | 13.7938 |
| NeighShrinkSure[54] | 28.1952 | 24.0840 | 20.2951 | 18.9744 | 15.4752 | 13.9918 |
| DWT-Cauchy[73] | 27.8005 | 23.5718 | 20.4775 | 18.7584 | 15.6785 | 13.8244 |
| DWT-NIG [75] | 28.1997 | 25.1846 | 22.7655 | 18.9872 | 15.9277 | 13.9274 |
| DST-NIG-WS | 28.8607 | 26.4988 | 24.5164 | 19.5803 | 16.5470 | 14.1226 |
| SNIGS-MAP (Proposed) | 29.6821 | 27.2180 | 25.9690 | 19.7350 | 16.5752 | 14.1574 |

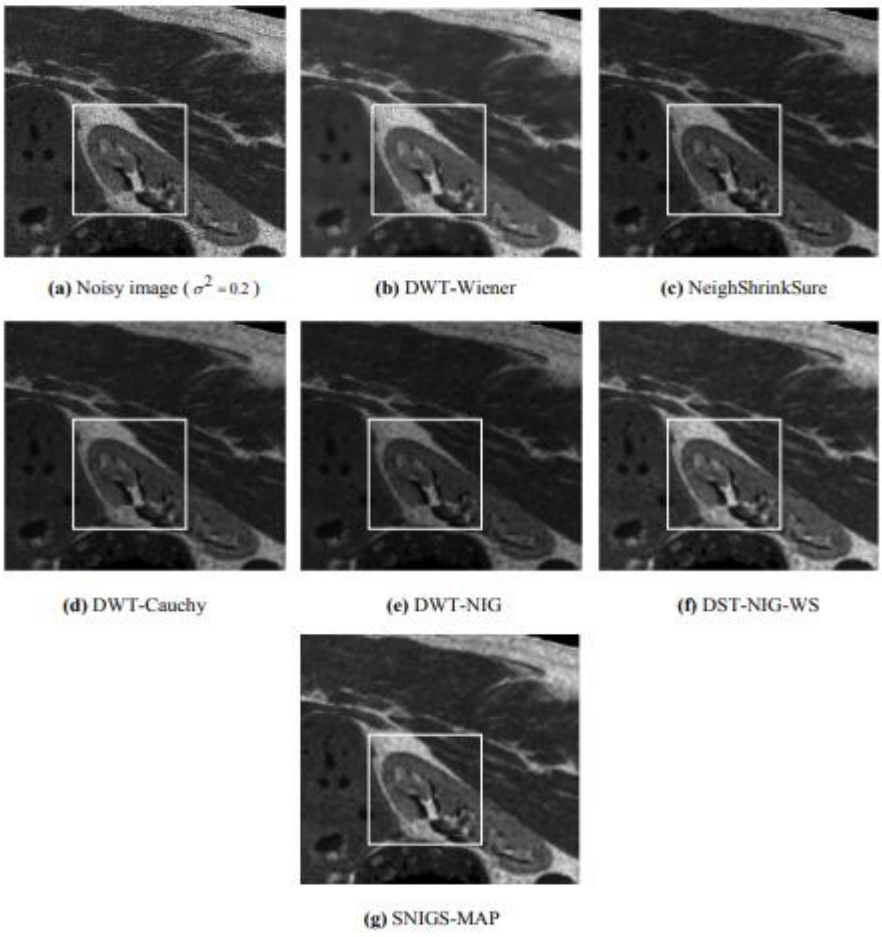


**Figure 2: Synthetic kidney ultrasound denoised images obtained from various denoising methods**

US pictures of a synthetic kidney acquired with different despeckling techniques are shown in Figure 2(a)-(2(g). The synthetic kidney US picture with a noise variance of 0.2 is shown in Figure 2(a). The area from which speckle noise may be efficiently eliminated is indicated by the white rectangle. Qualitative examination of the reconstructed pictures demonstrates that the quality of the image acquired using the proposed filter, i.e. the SNIGS-MAP filter, is superior to that of images obtained using other current filters. The image reconstruction utilising the SNIGS-MAP filter brings up sharp details and clean edges. When it comes to preserving small details in a picture, the DWT-Wiener filter yields the lowest quality results. Both the DWT-Cauchy filter and the DWT-NIG filter provide results of very comparable quality. Images produced with this filter are somewhat darker than those acquired with the DWT-Wiener filter, but they preserve finer details better. Images captured using the DST-NIG-WS filter have the highest levels of speckle suppression and edge retention compared to the other compared filters, but they are less visually appealing than those captured with the SNIGS-MAP filter.

## Conclusion

Focusing on strong denoising in homogenous areas while preserving fine features and edges along with vital image information, this paper sets out to design some unique spatial and transform domain filters that are useful in better denoising of medical US pictures. It is suggested to use two spatial domain filters and three transform domain filters. Experiments were performed on both synthetic and real-world US pictures using all of the suggested filters. The computational programme RMATLAB 2014a is used for all the simulation work. The Field-II programme was used to create the synthetic ultrasound pictures, while actual ultrasound images were obtained from a legitimate ultrasound image database. All of the recommended filters are tested, ranked, and compared to industry leaders to see which offers the greatest overall performance. PSNR, SNR, EKI, SSIM, FOM, and CC are used for quantitative evaluation of synthetic US pictures. However, for true US pictures, MVR and ENL have been treated as standard parameters for quantitative assessment since no noise-free true US image was provided. Different denoising filters' output denoised pictures are compared for quality of denoising and edge preservation.

## References

1. X. Lang, B. He, Y. Zhang, Q. Chen and L. Xie, "Adaptive Clutter Filtering for Ultrafast Doppler Imaging of Blood Flow Using Fast Multivariate Empirical Mode Decomposition," *2021 IEEE International Ultrasonics Symposium (IUS)*, Xi'an, China, 2021, pp. 1-4, doi: 10.1109/IUS52206.2021.9593919
2. N. Laroche, S. Bourguignon, J. Idier, E. Carcreff and A. Duclos, "Fast Non-Stationary Deconvolution of Ultrasonic Beamformed Images for Nondestructive Testing," in *IEEE Transactions on Computational Imaging*, vol. 7, pp. 935-947, 2021, doi: 10.1109/TCI.2021.3107977.
3. I.Taghavi *et al*., "Automatic Classification of Arterial and Venous Flow in Super-resolution Ultrasound Images of Rat Kidneys," *2021 IEEE International Ultrasonics Symposium (IUS)*, Xi'an, China, 2021, pp. 1-3, doi: 10.1109/IUS52206.2021.9593655

4. K. Christensen-Jeffries, O. Couture, P. A. Dayton, Y. C. Eldar, K. Hyny-nen, F. Kiessling, M. O'Reilly, G. F. Pinton, G. Schmitz, M. Tang et al., "Super-resolution ultrasound imaging", Ultrasound Med. Biol., vol. 46, no. 4, pp. 865-891, 2020
5. S. B. Andersen, I. Taghavi, C. A. V. Hoyos, S. B. Søgaard, F. Gran, L. Lonn, et al., "Super-resolution imaging with ultrasound for visualization of the renal microvasculature in rats before and after renal ischemia: A pilot study", Diagnostics, vol. 10, no. 11, pp. 862, 2020
6. J. A. Jensen, S. B. Andersen, C. A. V. Hoyos, K. L. Hansen, C. M. Sørensen and M. B. Nielsen, "Tissue motion estimation and correction in super resolution imaging", Proc. IEEE Ultrason. Symp., pp. 1-4, 2019.
7. R. Nayak, V. Kumar, J. Webb, M. Fatemi and A. Alizad, "Non-invasive small vessel imaging of human thyroid using motion-corrected spatiotemporal clutter filtering", *Ultrasound in medicine & biology*, vol. 45, no. 4, pp. 1010-1018, 2019
8. J. Tierney, J. Baker, D. Brown, D. Wilkes and B. Byram, "Independent component-based spatiotemporal clutter filtering for slow flow ultrasound", *IEEE transactions on medical imaging*, vol. 39, no. 5, pp. 1472-1482, 2019
9. O. Solomon, R. Cohen, Y. Zhang, Y. Yang, Q. He, J. Luo, et al., "Deep unfolded robust PCA with application to clutter suppression in ultrasound", IEEE transactions on medical imaging, vol. 39, no. 4, pp. 1051-1063, 2019
10. J.E. Tierney, D.M. Wilkes and B.C. Byram, "Independent component analysis-based tissue clutter filtering for plane wave perfusion ultrasound imaging" in In Medical Imaging 2019: Ultrasonic Imaging and Tomography, International Society for Optics and Photonics, vol. 10955, pp. 1095503, March. 2019
11. J. Baranger, B. Arnal, F. Perren, O. Baud, M. Tanter and C. Demené, "Adaptive spatiotemporal SVD clutter filtering for ultrafast Doppler imaging using similarity of spatial singular vectors", IEEE transactions on medical imaging, vol. 37, no. 7, pp. 1574-1586, 2018.
12. P. Song, J.D. Trzasko, A. Manduca, B. Qiang, R. Kadirvel, D.F. Kallmes, et al., "Accelerated singular value-based ultrasound blood flow clutter filtering with randomized singular value decomposition and randomized spatial downsampling", IEEE transactions on ultrasonics ferroelectrics and frequency control, vol. 64, no. 4, pp. 706-716, 2017.
13. P. Song, A. Manduca, J.D. Trzasko and S. Chen, "Ultrasound small vessel imaging with block-wise adaptive local clutter filtering", IEEE transactions on medical imaging, vol. 36, no. 1, pp. 251-262, 2016.
14. R. Otazo, E. Candes and D.K. Sodickson, "Low - rank plus sparse matrix decomposition for accelerated dynamic MRI with separation of background and dynamic components", Magnetic resonance in medicine, vol. 73, no. 3, pp. 1125-1136, 2015
15. I.K. Ekroll, M.M. Voormolen, O.K.V. Standal, J.M. Rau and L. Lovstakken, "Coherent compounding in doppler imaging", IEEE transactions on ultrasonics ferroelectrics and frequency control, vol. 62, no. 9, pp. 1634-1643, 2015.